Experimental Realization of a New Type of Crystalline Undulator

Tobias N. Wistisen, Kristoffer K. Andersen, Serdar Yilmaz, Rune Mikkelsen,
John Lundsgaard Hansen, and Ulrik I. Uggerhøj
Department of Physics and Astronomy, Aarhus University, 8000 Aarhus, Denmark

Werner Lauth and Hartmut Backe
Institut für Kernphysik, Johannes Gutenberg Universität Mainz, 55099 Mainz, Germany
(Received 15 March 2014; published 24 June 2014)

A new scheme of making crystalline undulators was recently proposed and investigated theoretically by Andriy Kostyuk, concluding that a new type of crystalline undulator would be not only viable, but better than the previous scheme. This article describes the first experimental measurement of such a crystalline undulator, produced by using $Si_{1-x}Ge_x$-graded composition and measured at the Mainzer Microtron facility at beam energies of 600 and 855 MeV. We also present theoretical models developed to compare with the experimental data.

DOI: 10.1103/PhysRevLett.112.254801 PACS numbers: 41.60.-m, 61.50.Ah, 61.85.+p

There is great interest in the investigation of crystalline undulators, both theoretically and experimentally (see, e.g., [1–3]). We present here a measurement carried out on a new type of crystalline undulator that shows promise as a source of high-energy, sharp spectral distribution, tunable source of incoherent radiation. We present also different theoretical models of varying complexity to describe the measurements and use these models to suggest improvements for future experiments. The inspiration for doing this experiment was provided by the theoretical proof of feasibility, as shown in [4]. The usual schemes of making crystalline undulators involve some method of bending the planes or axes of the crystal, altering the usual channeling motion (see [5] for a review of channeling and related phenomena). One scheme, the large-amplitude, large-period, bends the planes such that the bending amplitude and period of the planes are significantly larger than the amplitude and period of the channeling motion. The new scheme consists of having a short-amplitude, short-period configuration, meaning that the predominant motion is still channeling motion, in contrast to the large-amplitude, large-period regime. In the short-amplitude, short-period regime, the bending of the planes only slightly perturbs the channeling motion trajectory, leading to increased radiation emission at higher photon energies than the usual channeling radiation.

We use units where $\hbar = c = 1$ and $e^2 = \alpha \simeq (1/137)$, unless otherwise stated. The crystal was grown in the [001] direction by the method of molecular beam epitaxy at Aarhus University. This method makes it possible to grow a crystal with a varying concentration of different elements as a function of time. This crystal was grown with a mixture of Si and Ge with a concentration of Ge following a triangle function. The crystal has a thickness of 3 μm of which the last 0.1 μm is pure Si. The following relation [6] can be found between the amplitude of the bending of the [110] plane a_u, the undulator wavelength λ_u, and the average germanium concentration $\bar{\chi}$. Here the concentration is the ratio of number of Ge atoms per volume to the total number of atoms per volume:

$$\bar{\chi} \simeq 170 \frac{a_u}{\lambda_u}. \tag{1}$$

The crystal was made with roughly 10 periods along the (110) plane, which results in $\lambda_u = 0.41$ μm. This value was later measured using a Rutherford backscattering method on the sample giving a value of $\lambda_u = 0.43 \pm 0.004$ μm. The minimum and maximum values of the Ge concentration were $(0.3 \pm 0.1)\%$ and $(1.3 \pm 0.1)\%$, respectively. Equation (1) is for the case when the lower concentration is 0%. In our case, we should use $\bar{\chi} = (0.50 \pm 0.14)\%$, giving an amplitude of $a_u = 0.12 \pm 0.034$ Å.

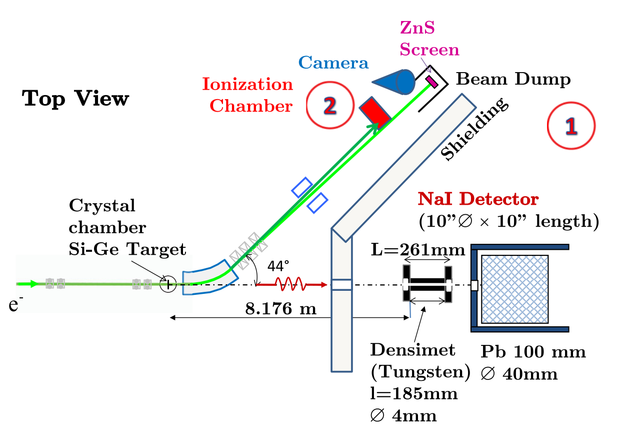

FIG. 1 (color online). The experimental setup. The electron beam enters the crystalline target before being bent away by the first magnet. The emitted radiation travels through the collimator and is detected by an NaI detector.

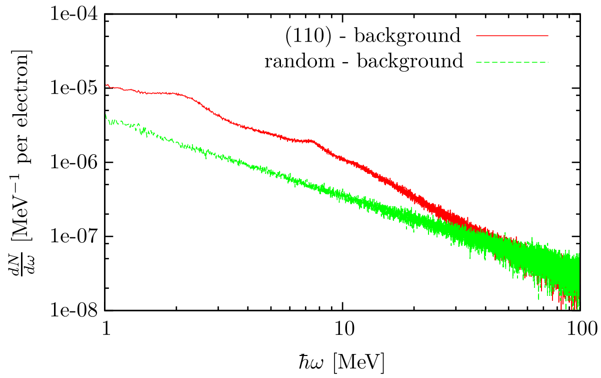

FIG. 2 (color online). The photon number spectra for channeling along the (110) plane and particle penetration in a random orientation, subtracted the background for the 600-MeV data.

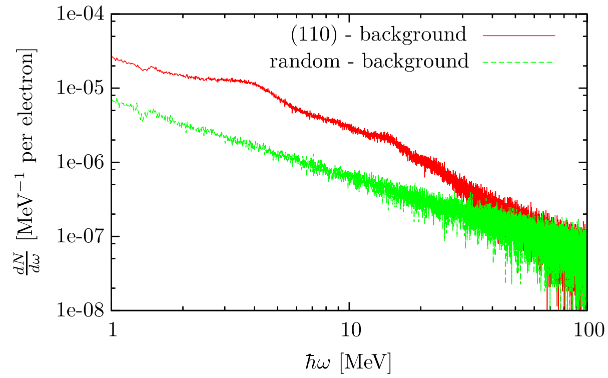

FIG. 3 (color online). The photon number spectra for channeling along the (110) plane and particle penetration in a random orientation, subtracted the background for the 855-MeV data.

The experiment was conducted at the Mainzer Microtron. Figure 1 shows the experimental setup. A well-collimated electron beam enters the crystalline target and is afterward deflected by the first magnet. The emitted radiation travels through the collimation system and is detected by a NaI detector. The beam entered the crystal along the (110) plane but avoided any direction of axial symmetry. An off-plane measurement was made by turning the crystal as to avoid any crystal symmetry directions, as well as a measurement of the background. A linear energy calibration was made based on the known peaks in the background from radioactive decays and by using radioactive sources. Measurements were performed at beam electron energies of 600 and 855 MeV, as illustrated in Figs. 2 and 3. The case of 600-MeV electron energy consists of a 3000-s measurement, while the 855-MeV electron energy is 1000 s. At 600 MeV, the largest rms beam spot size was measured to be 138 μm, and the largest rms divergence to be 176 μrad. At this energy, the Lindhard critical angle is $\theta_c = 340\ \mu$rad. The beam current was 3 ± 0.6 pA.

For theoretical comparison and predictions for future experiments, we have developed theoretical models based on a numerical solution of the classical equations of motion and radiation emission. A simple model of channeling motion uses a continuum potential, a smooth potential obtained by averaging over the potential of each individual atom in the crystal along a direction of symmetry. The radiation emitted by a particle is found by first calculating the classical trajectory of the particle and then using the classical formula for emission of radiation. The trajectory is found from the relativistic Newton's 2nd law $\frac{d\vec{p}}{dt} = -\nabla U$, where U is the potential energy and $\vec{p} = \gamma m \vec{v}$ the relativistic momentum. The emitted energy during time T is given differentially in photon energy and solid angle by [7]

$$\frac{d^2E}{d\omega d\Omega} = \frac{\alpha}{4\pi^2}\left|\int_0^T \frac{\mathbf{n}\times[(\mathbf{n}-\boldsymbol{\beta})\times\dot{\boldsymbol{\beta}}]}{(1-\boldsymbol{\beta}\cdot\mathbf{n})^2} e^{i\omega(t-\mathbf{n}\cdot\mathbf{r}(t))}dt\right|^2, \quad (2)$$

where $\mathbf{n}$ is the direction of observation, $\mathbf{r}(t)$ is the particle trajectory, and $\boldsymbol{\beta} = \dot{\mathbf{r}}(t)$ is the velocity vector. The relation between the emitted energy dE and the number of photons dN is $dE = \hbar\omega dN$. A classical calculation is justified at high beam energies. As the number of states of the transverse motion increases, the classical motion is recovered. Consider, for instance, a simple harmonic well, bounded by some upper energy U_0, the potential depth. The energy separation between states in the harmonic oscillator with potential $U(x) = (1/2)m\omega^2x^2$ is $\Delta E = \omega$; therefore, the number of states is $N_0 = U_0/\omega$. Suppose that we now have a particle with a relativistic energy $E = \gamma m$ that penetrates the crystal. In the rest frame of the particle, the potential is transformed as $U \to \gamma U$ and so $\omega \to \sqrt{\gamma}\omega$. The number of states therefore becomes $N = (\gamma U_0/\sqrt{\gamma}\omega) = \sqrt{\gamma}N_0$. N_0 is of the order of 1, and therefore, a classical calculation is justified when $\sqrt{\gamma} \gg 1$, which is the case in this experiment.

We performed the calculation for two potentials, one of which was a continuum planar potential given by [8]

$$U(x) = V[\cosh(\delta(\sqrt{1+\eta^2} - \sqrt{y^2+\eta^2})) - 1], \quad (3)$$

with $V = 3.5$ eV, $\delta = 2.9$, $\eta^2 = 0.0045$, and $y = 2x/d_{pl}$ with $d_{pl} = 1.92$ Å. The other potential used was a sum over the potential from each individual atom in the lattice:

$$U(\vec{r}) = \sum_i U_a(\vec{r} - \vec{r}_i), \quad (4)$$

where the summation is over a diamond cubic lattice. The atomic potential used is

$$U_a(r) = \frac{Z\alpha}{r}\varphi\left(\frac{r}{a}\right), \quad (5)$$

where $\varphi(r/a)$ is a Thomas-Fermi screening function and $a = 0.8853a_0Z^{-(1/3)}$ is a screening length. The screening function is approximated by the Molière formula [9]

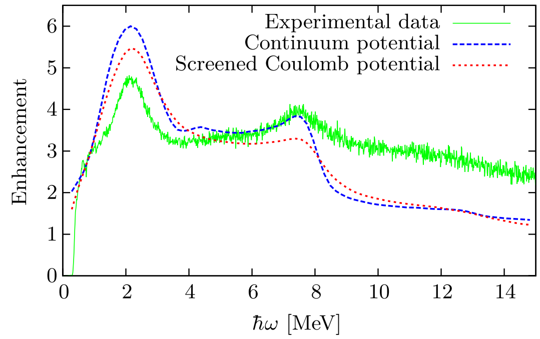

FIG. 4 (color online). Comparison of theoretical and experimental radiation yield for the 600-MeV data.

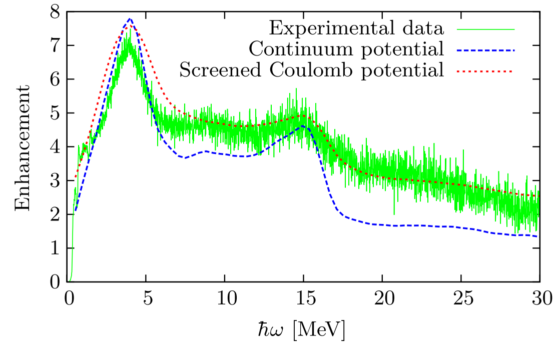

FIG. 5 (color online). Comparison of theoretical and experimental radiation yield for the 855-MeV data.

$$\varphi\left(\frac{r}{a}\right) = \sum_{i=1}^{3} \alpha_i e^{-\frac{\beta_i r}{a}},$$

with coefficients $\{\alpha_i\} = \{0.1, 0.55, 0.35\}$ and $\{\beta_i\} = \{6.0, 1.2, 0.3\}$. Furthermore, the atomic positions were displaced in a random direction by sampling a three-dimensional Gaussian distribution to simulate thermal vibrations with an rms amplitude of $u = 0.062$ Å [10]. The model used to describe the potential of the periodically bent plane due to the periodic addition of germanium is given by

$$U_{bent}(x, y, z) = U(x, y - a_u \sin(k_u z + \varphi), z). \quad (6)$$

The beam direction is chosen to be the z direction and the direction of channeling oscillation as the y direction; i.e., the potential center follows the path $a_u \sin(k_u z + \varphi)$.

In order to get accurate values for comparison with the experiment, Eq. (2) must be integrated over the relevant angular region, depending on the collimation setting in the experiment. Only calculating the emission in the exactly forward direction as is done in [6] does not suffice for experimental comparison. The radiation was calculated on an angular (Cartesian) grid of 20×20 points as this produced converged results.

The two potentials described both have their advantages and disadvantages. The continuum potential model allows for a fast numerical calculation, which gives good results in reasonable agreement with the experiment, but it is well known that this does not account for the Bethe-Heitler bremsstrahlung, which is usually added to the radiation from the channeling motion. The calculation using the full potential of Eq. (4) is considerably slower because the step size when solving the system of differential equations for the trajectory cannot be larger than the typical scale of the variation of the potential, which is less than the size of the atom. It is nontrivial to determine the exact amount of Bethe-Heitler radiation, which should be added with this type of undulator crystal. Furthermore, the continuum potential does not take into account the dechanneling process. The more elaborate potential was chosen to deal with these issues, where both Bethe-Heitler bremsstrahlung and dechanneling are inherently included. For the continuum potential, we have added the Bethe-Heitler bremsstrahlung, as measured in the random crystal orientation to the calculated result.

A direct fit of the data in the random direction with the Bethe-Heitler formula (see, e.g., [5]) shows that experimental values are too low by factors of 15.5 and 8.5 at 600 and 855 MeV, respectively. This is mainly due to an angular collimation performed in the experiment where the opening angle was 0.49 mrad corresponding to angles less than $0.28/\gamma$ and $0.40/\gamma$ from the central axis for 600 and 855 MeV, respectively. Classical works (such as [7]) show that at relativistic electron energies and low photon energies $\omega \ll E$, the angular distribution of the intensity of bremsstrahlung is independent of the photon energy ω, barring small corrections. The normalized angular distribution is given as

$$\frac{dI}{d\Omega} = \frac{3\gamma^2}{2\pi} \frac{1 + \gamma^4\theta^4}{(1 + \gamma^2\theta^2)^4}, \quad (7)$$

where dI is the differential probability of emission within the solid angle $d\Omega$. Integrating this up to the two angular regions stated gives an expected reduction of 9.85 and 5.53 for 600 and 855 MeV, respectively. In both cases, this means that a factor of about ~1.5 is unaccounted for. This error is reasonable considering the uncertainty on the beam current and the fact that a slight misalignment of the collimator would further decrease the solid angle of the detected radiation. Considering the size of the multiple scattering angle of 0.134 mrad at 600 MeV after traversing the target suggests that this might also have a small effect. The normalization procedure for the theoretical curves is to multiply with the same factor as is necessary for the fit with the Bethe-Heitler formula. We also note that in the simulations a value of $a_u = 0.13$ Å was used, which is well within the experimental uncertainty. It is seen in

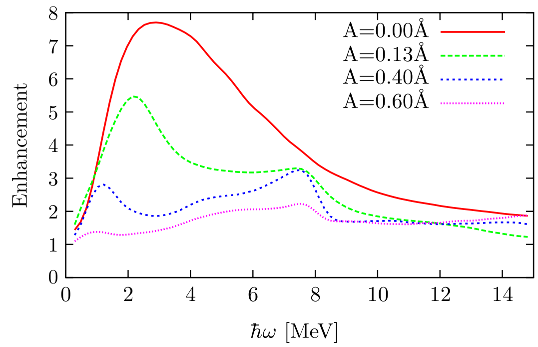

FIG. 6 (color online). Calculated radiation spectra for different values of the bending amplitude a_u at 600-MeV electron energy using the screened Coulomb potential.

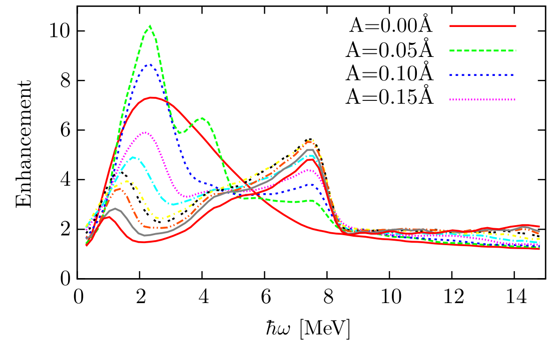

FIG. 7 (color online). Calculated radiation spectra for different values of the bending amplitude a_u at 600-MeV electron energy using the continuum potential. The bending amplitude goes from 0 Å to 0.45 Å in steps of 0.05 Å.

simulations [see Fig. (6)] that the position of the channeling peak in energy moves with varying bending amplitude.

This value of a_u was therefore chosen for good agreement of the channeling peak position, although it makes only a minor difference in comparison to using $a_u = 0.12$ Å [see Figs. (4)and (5) for a comparison of theory to the experiment]. Enhancement is the ratio of the total radiation spectrum to the Bethe-Heitler spectrum. The leftmost peaks stem from channeling and the rightmost from the undulator motion. The position of the undulator peak considering just forward emission of radiation should be at $2\gamma^2 k_u$, with $k_u = 2\pi/\lambda_u$, which agrees well with the experiment. The size of the peaks, however, does disagree significantly. Attributing the factor of ~1.5 of deviation in the bremsstrahlung yield to a slight misalignment of the collimator could explain the deviation of the radiation in the aligned case as well. As the collimation angle becomes very narrow in units of $1/\gamma$, the spectral distribution can change significantly, and a misalignment will be more pronounced. For 855 MeV, the collimation is not quite as narrow in units of $1/\gamma$, and therefore, we have better agreement.

In conclusion, we remark that the overall agreement between experiment and theory is good. There is a definite crystalline undulator effect caused by the bending of the planes, as can be seen by comparing with the regular channeling spectrum, as seen in Fig. (6).

Nevertheless, this crystal has a relatively low value of a_u compared with those considered in [6]. This, along with the fact that the calculations in [6] are for the exactly on-axis emission, means that the undulator peak seen in the experiment is not as pronounced. The simulations we have performed for other values of the bending amplitude a_u, as seen in Figs. (6) and (7), are integrated over a collimation angle of $1/\gamma$, but otherwise with the same parameters as in the experiment. Here it is seen that it is unlikely that the undulator peak will become larger in absolute size by increasing the bending amplitude of the planes, but a relative increase to the rest of the spectrum can be achieved, which would be desirable. It should also be noted that for larger values of a_u the continuum potential exaggerates the undulator effect in comparison to using the screened Coulomb potential, as can be seen by comparing Figs. (6) and (7). A surprising result is the effect on the shape of the channeling peak. For electrons, the channeling radiation spectrum is usually very broad in contrast to the narrow spectral distribution seen here in both the experiment and simulations. These experiments and our simulations therefore show that if the goal is to achieve a narrow spectral distribution it might also be worthwhile to investigate small values of a_u, like 0.05 Å or 0.1 Å at 600 MeV, such that these oscillations serve only to disturb the formation of channeling radiation, making it spectrally more narrow, as seen in Fig. (7).

We thank Allan H. Sørensen (AU) for helpful discussions in regards to the theoretical simulations and Robert Noble (SLAC) for reading and commenting on the manuscript.

[1] W. G. A. V. Korol and A. V. Solov'yov, *Channeling and Radiation in Periodically Bent Crystals* (Springer, New York, 2013).
[2] U. Mikkelsen and E. Uggerhøj, Nucl. Instrum. Methods Phys. Res., Sect. B **160**, 435 (2000).
[3] V. Baryshevsky and V. Tikhomirov, Nucl. Instrum. Methods Phys. Res., Sect. B **309**, 30 (2013).
[4] A. Kostyuk, Phys. Rev. Lett. **110**, 115503 (2013).
[5] U. I. Uggerhøj, Rev. Mod. Phys. **77**, 1131 (2005).
[6] A. Kostyuk, arXiv:1301.4491.
[7] J. D. Jackson, *Classical Electrodynamics* (John Wiley & Sons Inc., New Jersey, 1991), 3rd ed.
[8] V. Baier, V. Katkov, and V. Strakhovenko, *Electromagnetic Processes at High Energies in Oriented Single Crystals* (World Scientific, Singapore, 1998).
[9] D. S. Gemmell, Rev. Mod. Phys. **46**, 129 (1974).
[10] M. L. Ter-Mikaelian, *High-Energy Electromagnetic Processes in Condensed Media* (Wiley-Interscience, New York, 1972).